


Research Article

Gray-white matter contrast as an index of neurobiological alterations in anorexia nervosa[☆]

Sanberk Ugur^a, Christopher R. Madan^b, Valentina Meregalli^a, Sofia Gentili^a,
 Serena Giovannini^a, Marco Romanelli^a, Renzo Manara^{a,c}, Angela Favaro^{a,c},
 Enrico Collantoni^{a,c,*} 

^a Department of Neuroscience, University of Padua, Padova, Italy

^b School of Psychology, University of Nottingham, Nottingham NG7 2RD, UK

^c Padua Neuroscience Center, University of Padua, Padova, Italy

ARTICLE INFO

Keywords:

Eating disorders
 Anorexia nervosa
 Neuroimaging
 Cortical structure
 Gray-white matter contrast

ABSTRACT

This neuroimaging study sought to characterize differences in cortical gray-white matter contrast (GWC) between individuals with anorexia nervosa (AN) and age-matched healthy controls (HC) and compare these findings with conventional cortical thickness (CT) measures. The study included 58 female participants (29 AN, 29 HC). T1-weighted images were acquired using a 3 T scanner and processed with FreeSurfer. GWC maps were calculated at each cortical vertex. Vertex-wise general linear models assessed group differences in GWC controlling for age only, and controlling for age and vertex-wise CT. A separate model tested CT differences. Models were corrected for multiple comparisons using cluster-wise correction. Spearman correlations related mean GWC in significant clusters to BMI at scan, age at onset, and illness duration. The age-only model revealed two clusters in the left hemisphere with higher GWC in patients with AN, namely the inferior temporal cortex and medial orbitofrontal cortex. No clusters survived in the model controlling for age and CT. The CT analysis revealed no significant group differences. Mean GWC in clusters did not correlate with clinical severity indices in AN. Patients with AN exhibit focal increases in GWC despite the absence of detectable cortical thinning, suggesting that the GWC can provide complementary information in understanding the neurobiology of AN. The elimination of GWC differences when adjusting for CT likely reflects shared variance rather than true absence of effect. Lack of correlations with clinical indices may be due to limited sample size. Future longitudinal and multimodal studies are warranted to determine the underpinnings of GWC alterations.

Introduction

Anorexia nervosa (AN) is a severe psychiatric disorder that typically begins in adolescence, defined by persistent dietary restriction and significantly low body weight, and is associated with a considerable medical burden and functional impairment (American Psychiatric Association, 2013). Despite advances, the neurobiology of AN remains incompletely characterized (Treasure et al., 2020). Accordingly, in vivo structural neuroimaging has become central to delineating disorder-related brain alterations. Structural MRI studies examining both gray and white matter have consistently documented widespread, heterogeneous abnormalities (Seitz et al., 2013). These include global and regional reductions in cortical thickness, gyrification, and volume,

together with alterations in white matter volume and microstructural integrity (Collantoni et al., 2019, 2025; Meneguzzo et al., 2019). A large-scale multisite analysis from the ENIGMA consortium further reported widespread cortical-thickness reductions in AN, among the largest observed across psychiatric conditions, with effects that track nutritional status and partially normalize with weight restoration (Walton et al., 2022). Within the cortex, complementary morphometric indices reflect partly distinct biology: cortical thickness approximates dendritic/neuropil architecture; curvature and gyrification reflect developmental patterning; and intensity- or diffusion-based metrics are sensitive to myeloarchitecture (Fischl & Dale, 2000; Madan, 2018; White et al., 2010). Jointly modelling these features helps disentangle overlapping mechanisms and ground interpretation in a coherent

[☆] This article is part of a special issue entitled: 'Eating disorders' published in Neuroscience.

* Corresponding author at: Department of Neuroscience, University of Padua, Via Giustiniani, 2 - 35128 Padova, Italy.

E-mail address: enrico.collantoni@unipd.it (E. Collantoni).

pathophysiological framework. Moreover, when combined as morphometric similarity or structural covariance, they recapitulate constraints of the structural connectome and align with cytoarchitectonic and transcriptomic gradients, enabling network-level inference from standard MRI. In AN, multivariate morphometric similarity appears globally reduced and selectively disrupted in transmodal networks, scaling with nutritional status, supporting a connectome-constrained view in which local cortical alterations are embedded within large-scale network architecture (Facca et al., 2025).

Against this backdrop, the biological substrates of these macroscopic and network-level differences remain uncertain. Putative contributors, including dehydration and shifts in brain water content, synaptic and dendritic pruning, neuroinflammatory processes, and disrupted myelination, likely vary with illness stage and nutritional status (King et al., 2018). Conventional morphometric indices offer limited biological specificity, hindering the disambiguation and longitudinal tracking of these mechanisms. This motivates the use of alternative morphometric markers capable of providing complementary, non-redundant insights into brain structure (Collantoni et al., 2020, 2021). One such marker is gray-white matter contrast (GWC), derived from the relative signal intensity difference at the GM-WM boundary in T1-weighted MRI (Salat et al., 2009). GWC is believed to reflect microstructural properties at the cortical interface, particularly intracortical myelin content and cytoarchitectural differentiation, and varies systematically across typical development and aging, tracking maturation of cortical myeloarchitecture and predicting chronological age and cognitive performance (Drakulich et al., 2021; Lewis et al., 2018; Salat et al., 2009). In clinical populations, schizophrenia-spectrum studies report increased GWC in highly myelinated sensory-motor cortices and exposure-related decreases in first-episode cases, whereas autism spectrum disorder is characterized by overall reductions in GWC with age-dependent effects most pronounced in youth (Chwa et al., 2020; Jørgensen et al., 2016; Mann et al., 2018). Importantly, GWC exhibits marked regional variation across the lifespan, with developmental trajectories that mirror intracortical myelination and cortical maturation. Given the typical onset of AN during adolescence, a critical period for cortical development, GWC may serve as a particularly informative index for investigating subtle disruptions in cortical organization and myeloarchitecture associated with the disorder. In light of converging evidence for altered cortical microstructure and myelination in AN, as well as widespread but heterogeneous cortical thinning and volumetric changes, we considered it plausible that individuals with acute AN might show increased GWC relative to healthy controls, reflecting exaggerated gray-white matter signal differences at the cortical boundary. Because GWC is only partially correlated with cortical thickness, we further anticipated that any group differences in GWC could be at least partly independent of local CT, thereby offering complementary information on cortical microstructure beyond conventional morphometric indices. Associations between regional GWC alterations and clinical variables (BMI, age at onset, illness duration) were examined in an explicitly exploratory and non-directional manner. In this context, we present a preliminary investigation of GWC in a cohort of individuals with AN compared to healthy controls (HC), with the aim of evaluating its potential as a morphometric marker that may complement existing findings on brain structure in this complex condition.

Method

Participants

Fifty-eight female participants were included in the study: 29 individuals with acute AN and 29 HCs. Only females were included due to the very low prevalence of male patients and to avoid potential confounding factors. Patients with AN were consecutively recruited from the Padua Eating Disorders Unit and met DSM-5 criteria (American Psychiatric Association, 2013). HCs were matched for ethnicity,

educational level, and handedness, and were screened to exclude any personal or first-degree family history of psychiatric disorders, including eating disorders. Exclusion criteria for both groups included male sex, history of head trauma, major neurological or systemic illness, pregnancy, psychotic or bipolar disorders, substance abuse, intellectual disability, and any contraindication to MRI. All MRI examinations were obtained at baseline in the acute stage of illness. Patients were scanned either at admission to the partial-hospitalization program, prior to intensive nutritional rehabilitation, or during outpatient care. Weights were stable on chart review, with no documented weight restoration and week-to-week fluctuations within routine measurement variability (typically < 1 kg or <0.3 BMI units). No patient was in recovery at the time of scanning. All participants provided written informed consent, and the study was approved by the Ethics Committee of the Hospital of Padova (N° 1598P).

MRI Acquisition

Each participant underwent a complete MR scan using a 3 T MRI scanner (3 Tesla Philips Ingenia) with a 32-channel quadrature head coil. Each participant underwent a whole-brain 3D-T1 magnetization-prepared rapid gradient-echo sequence in the sagittal plane with the following parameters: TR/TE = 6676 ms/3 ms, FOV = 240 mm; flip-angle = 8°, resolution = 1.0 × 1.0 × 1.0 mm³; number of slices = 181. MRI sessions were scheduled approximately 2 h after a main meal to promote comfort and minimize immediate post-prandial effects. No hardware upgrade occurred during the study period, and quality control was performed to assess image artifacts or motion effects prior to preprocessing.

Image processing and GWC computation

T1-weighted images were processed with *FreeSurfer* v7.4.1 (Fischl, 2012). The recon-all pipeline was applied to perform intensity normalization, skull stripping, tissue segmentation, and surface reconstruction. All surfaces were visually inspected and manually corrected when needed. Gray-white matter contrast (GWC) was computed using the *ptsurfcon* tool based on normalized intensity volumes (*norm.mgz*), using the following formula:

$$\text{GWC} = 100 \times (\text{WM} - \text{GM}) / ((\text{WM} + \text{GM}) / 2)$$

Higher GWC values indicate greater signal intensity difference at the GM-WM boundary and are interpreted as proxies of intracortical myelin content (Chwa et al., 2020). Individual GWC maps were projected onto the *fsaverage* template and smoothed with a 15-mm FWHM Gaussian kernel.

To qualitatively illustrate this signal difference, Fig. 1 shows two representative coronal slices from individual participants with high and low GWC values, respectively.

Statistical analysis

Group-level statistical analyses of gray-white matter contrast (GWC) and cortical thickness (CT) were performed using *FreeSurfer*'s general linear modeling tools (*mri_glmfit*, *mri_glmfit-sim*). Each participant's GWC and CT maps were projected to the *fsaverage* template and smoothed using a 15-mm full-width-at-half-maximum (FWHM) Gaussian kernel. Analyses were conducted separately for the left and right hemispheres.

Two general linear models (GLMs) were constructed for the GWC analyses.

- Model 1 included diagnosis as the main predictor and age as a covariate.

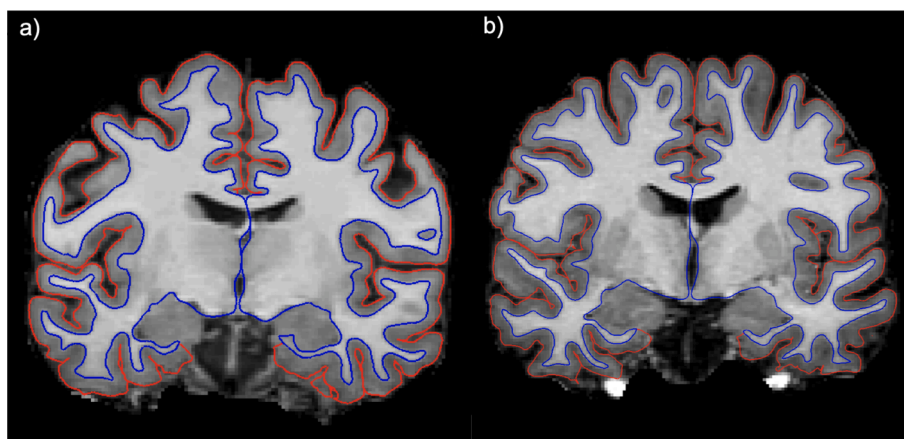


Fig. 1. Coronal slices from two representative participants showing low (a) and high (b) GWC. The signal intensity difference between white matter and adjacent gray matter is qualitatively greater in the high-GWC subject.

- Model 2 additionally included vertex-wise cortical thickness as a covariate, using FreeSurfer's per-voxel regressor (PVR) functionality. This method allows fine-grained statistical control for local cortical morphology, enabling the detection of GWC differences that are not attributable to regional cortical thinning.

A third model was constructed to assess differences in CT, including age as the sole covariate.

Statistical significance for all models was evaluated using cluster-wise correction for multiple comparisons based on Monte Carlo simulation (`mri_glmfit-sim` and `mri_surfcluster`). This approach employed a precomputed null-z distribution (CSD) with 10,000 simulations to estimate the probability of cluster occurrence under the null hypothesis. A cluster-forming threshold of $|t| > 2.00$ was used (equivalent to $p < 0.05$, two-sided), and clusters were considered significant if they survived a cluster-wise probability (CWP) threshold of 0.05. Anatomical labels for significant clusters were assigned according to the Desikan–Killiany atlas.

All cortical reconstructions and surface-based visualizations used to construct the figures were generated with FreeSurfer and displayed using its Freeview module. Mean GWC values were computed across all vertices within each significant cluster for each subject. This process was automated using custom MATLAB scripts, which incorporated SurfStat (Worsley et al., 2009) functions to read and process the FreeSurfer surface data files (.mgf). Box plots of mean GWC values for the significant clusters were made to show the inter-individual variance across groups. These subject-wise regional values were subsequently exported and used in statistical correlation analyses.

Within the AN group, Spearman's rank correlation coefficients (ρ) were calculated between cluster-level mean GWC and clinical indices including BMI at scan, age of onset, and illness duration. These analyses were conducted in IBM SPSS Statistics (version 26) and were considered exploratory; therefore, uncorrected p-values were reported with a threshold of significance set at $p < 0.05$.

Results

Participants

Twenty-nine patients with AN and twenty-nine healthy controls participated in the study. Among the patients with AN, 18 were enrolled in a day-hospital program and 11 were receiving outpatient treatment. Fifteen patients were undergoing pharmacological therapy: 7 were taking atypical antipsychotics, 10 antidepressants, and 2 benzodiazepines. The two groups did not differ in age; however, as expected, patients with AN showed a significantly lower BMI compared to healthy

controls (Table 1).

Vertex-wise differences in gray-white matter contrast: model 1

Vertex-wise analysis comparing AN and HC groups, controlling for age, revealed two clusters of significantly increased GWC in the left hemisphere in patients with AN (CWP < 0.05). Specifically, increased GWC was observed in the inferior temporal cortex (surface area: 1,386.7 mm², peak MNI: -43.1, -11.5, -36.9; CWP = 0.002) and the medial orbitofrontal cortex (surface area: 860.8 mm², peak MNI: -8.7, 48.2, -9.9; CWP = 0.03). See Figs. 2, 3, and 4 and Table 2.

Vertex-wise differences in gray-white matter contrast: model 2

The vertex-wise comparison between individuals with AN and HC, covarying for age and CT, revealed no clusters survived the cluster-wise correction for multiple comparisons. Visual inspection of the unthresholded statistical maps (Fig. 5) revealed spatial patterns similar to those observed in the age-only model, suggesting that the absence of significant clusters may be attributable to reduced statistical power following covariate adjustment rather than the complete absence of underlying group differences.

To investigate whether the attenuation of GWC effects in Model 2 was driven by local morphological collinearity, we extracted mean cortical thickness from the significant clusters identified in the age-adjusted model (Model 1) and assessed their relationship with GWC. Pearson's correlation analysis within the AN group revealed a significant positive relationship between mean GWC and cortical thickness in the medial orbitofrontal cluster ($r = 0.37$, $p = 0.049$). This suggests that shared variance likely contributed to the loss of significance in this region when controlling for thickness. In contrast, the inferior temporal cluster showed no significant correlation between GWC and thickness ($r = 0.09$, $p = 0.65$), indicating that GWC in this region captures microstructural information that is statistically independent of local cortical thickness.

Table 1

Participants' clinical and demographic characteristics.

	AN (N = 29) Mean (SD)	HC (N = 29) Mean (SD)	t (p)
Age (years)	22.97 (5.19)	25.21 (3.79)	-1.88 (0.066)
BMI (kg/m ²)	14.74 (3.18)	20.97 (1.79)	-8.69 (< 0.001)
Age of onset (years)	16.61 (3.37)		
Illness duration (months)	68.00 (62.23)		

AN, Anorexia Nervosa; HC, healthy control; BMI, Body Mass Index.

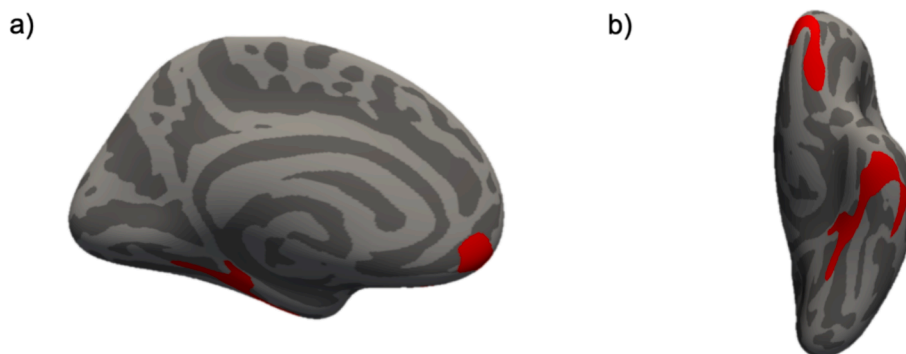


Fig. 2. Surface maps displaying significant clusters of increased GWC in patients with AN compared to HC, derived from the age-only model. Clusters are shown on the medial (a) and inferior (b) view of the left hemisphere.

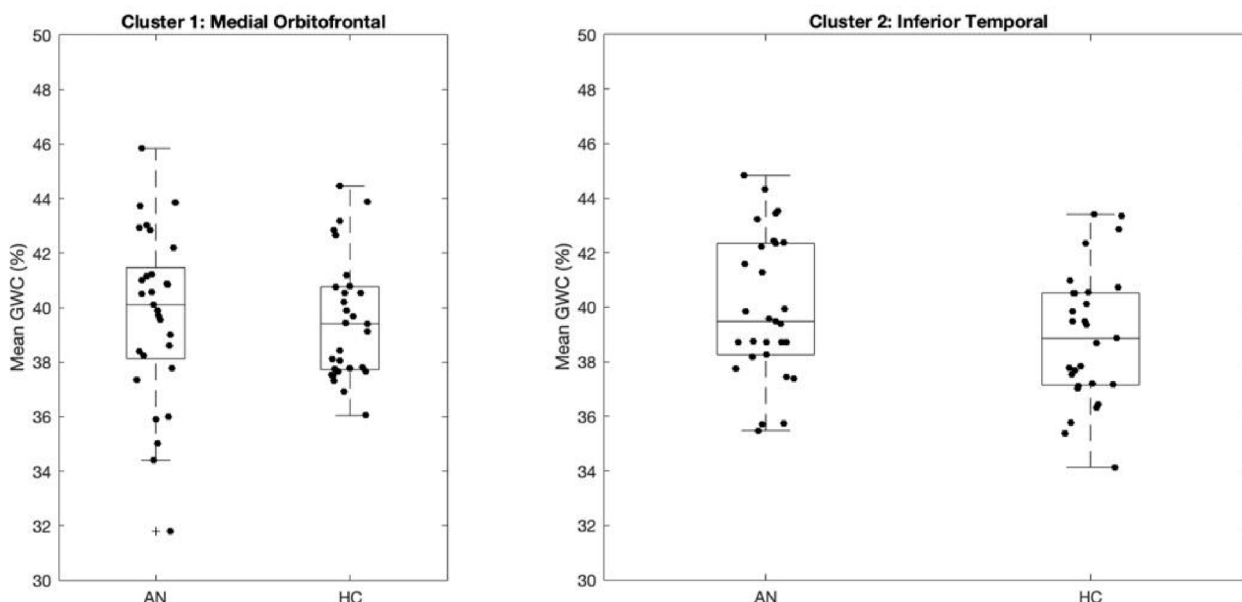


Fig. 3. Mean GWC values extracted from significant clusters identified in the left hemisphere in the AN > HC comparison (Model 1: age-adjusted). Boxplots display subject-wise mean GWC within the (a) medial orbitofrontal cortex and (b) inferior temporal cortex clusters, separately for patients with AN and HC. Black dots represent individual participant values; the box indicates the interquartile range, the line within the box denotes the median, and whiskers extend to $1.5 \times$ the interquartile range. Both clusters showed significantly increased GWC in the AN group after cluster-wise correction (CWP < 0.05).

Vertex-wise group differences in cortical thickness

The vertex-wise comparison of CT between individuals with AN and HC, covarying for age, revealed no clusters survived the cluster-wise correction for multiple comparison.

The corresponding unthresholded t-maps are displayed in Fig. 6 to aid qualitative interpretation.

Correlation with clinical variables

Preliminary analyses did not reveal significant correlations between GWC values and clinical severity indices. These findings should be interpreted with caution given the exploratory nature of the analysis and limited sample size. (Table 3).

Discussion

To the best of our knowledge, this is the first study to examine GWC in AN. We observed higher GWC in two anatomically and functionally distinct cortical regions in the left hemisphere: the medial orbitofrontal cortex and the inferior temporal cortex, among patients with AN relative

to HCs. Identified in the age-adjusted model, this pattern points to focal alterations at the gray-white matter boundary, which may reflect microstructural disruption associated with the disorder. Overall, the evidence is preliminary and hypothesis-generating. Mechanistically, pericortical contrast appears to capture variance beyond cortical thickness. Clinically, the work motivates testing whether GWC-based metrics track dimensions salient to AN (e.g., nutritional status, symptom burden, treatment response). An important methodological nuance in the interpretation of our findings lies in the divergence between the age-adjusted and CT-adjusted models. Specifically, the inclusion of CT as a vertex-wise covariate led to the attenuation of GWC differences below the threshold for cluster-wise significance. It's important to note that this attenuation is unlikely to reflect a true confounding effect of CT. In fact, our analyses did not identify any significant group differences in CT, either at the global or regional level. To clarify the role of shared variance, we conducted a cluster-wise correlation between GWC and CT. This analysis revealed distinct patterns: in the medial orbitofrontal cluster, we observed a significant positive correlation, confirming a degree of local collinearity that explains the loss of significance when controlling for CT. In stark contrast, the inferior temporal cluster showed no significant correlation. This provides evidence that, in the

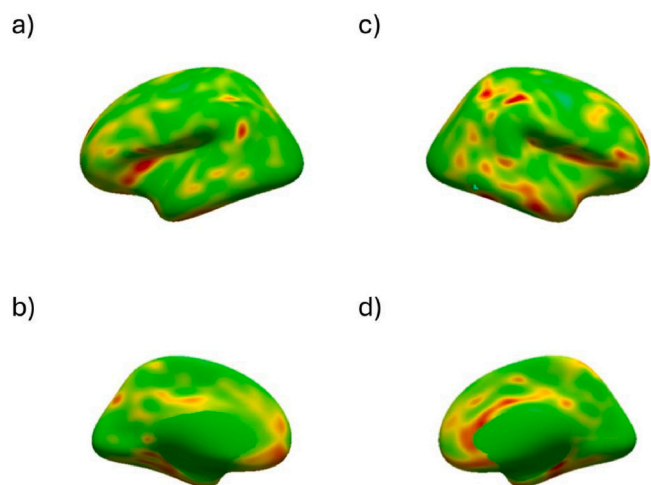


Fig. 4. Unthresholded vertex-wise statistical map of GWC differences between patients with AN and HC, adjusted for age. The surface maps display the full-range t-statistic distribution without cluster-wise correction (Model 1: age-adjusted). (a) Left hemisphere – lateral view, (b) Left hemisphere – medial view, (c) Right hemisphere – medial view, (d) Right hemisphere – lateral view.

Table 2
Cluster-wise results from the vertex-wise GWC comparison (AN > HC, age-only model).

Hemisphere	Anatomical Region	Cluster Size (mm ²)	Peak Vertex (MNI x,y,z)	CWP
Left	Inferior Temporal Cortex	1386.72	−43.1, −11.5, −36.9	0.002
Left	Medial Orbitofrontal Cortex	860.81	−8.7, 48.2, −9.9	0.030

The table reports hemisphere, anatomical label, surface area of the cluster (in mm²), cluster-wise p-value (CWP), and MNI coordinates of the peak vertex.

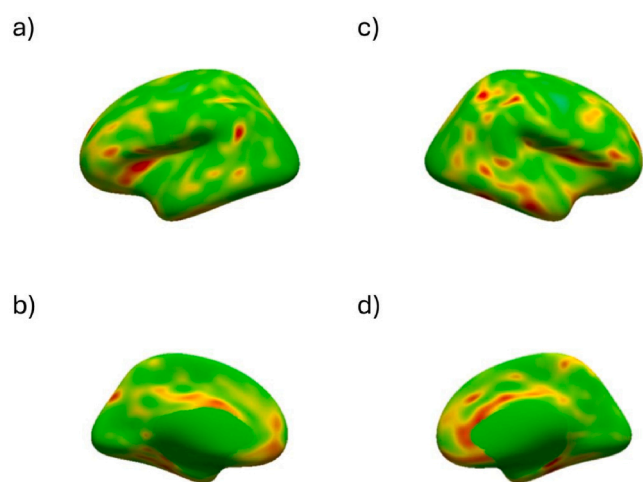


Fig. 5. Unthresholded vertex-wise statistical map of GWC differences between patients with AN and HC, adjusted for age and cortical thickness. The surface maps display the full-range t-statistic distribution without cluster-wise correction (Model 2: age and CT-adjusted). (a) Left hemisphere – lateral view, (b) Left hemisphere – medial view, (c) Right hemisphere – medial view, (d) Right hemisphere – lateral view.

inferior temporal cortex, GWC captures a microstructural signal that is statistically independent of local cortical thickness, and the loss of

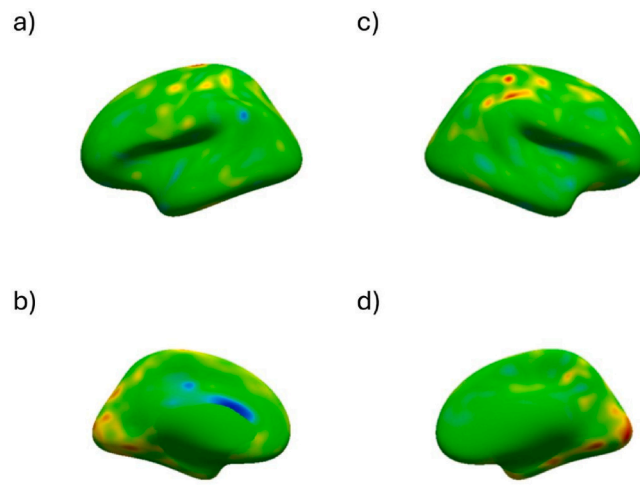


Fig. 6. Unthresholded vertex-wise statistical map of CT differences between patients with AN and HC, adjusted for age. The surface maps display the full-range t-statistic distribution without cluster-wise correction. (a) Left hemisphere – lateral view, (b) Left hemisphere – medial view, (c) Right hemisphere – medial view, (d) Right hemisphere – lateral view.

Table 3
Spearman’s correlations between cluster-wise GWC values and clinical variables in AN.

Variable	OFC Cluster (p)	IT Cluster (p)
BMI at scan	−0.05 (0.81)	−0.14 (0.50)
Age of onset	0.23 (0.24)	0.03 (0.89)
Illness duration	−0.31(0.11)	−0.01 (0.95)

significance in Model 2 in this region was likely a consequence of reduced statistical power or loss of degrees of freedom. Accordingly, we interpret the attenuation in the CT-adjusted model as primarily a statistical consequence of this shared variance and reduced sensitivity rather than evidence against microstructural differences, thereby underscoring the value of GWC as a complementary, microstructure-sensitive marker that may capture biology not indexed by cortical thickness. Consistent with this interpretation, GWC offers complementary sensitivity to GM–WM interface properties, such as intracortical myelination and local tissue composition, that are only weakly reflected in thickness measures (Madan, 2018). The increased GWC observed in patients with AN may reflect malnutrition-induced alterations at the gray-white matter interface, such as demyelination, reduced glial density, or shifts in water compartmentalization, that accentuate the signal intensity difference between cortical and subcortical tissue on T1-weighted MRI. These changes may occur even in the absence of overt morphological differences in cortical thickness, thereby highlighting the potential of GWC to capture subtle, physiologically meaningful tissue-level alterations.

The regions exhibiting increased GWC in patients with AN, the medial orbitofrontal cortex and the inferior temporal cortex, are critically involved in cognitive and perceptual processes relevant to the pathophysiology of the disorder. The OFC plays a pivotal role in reward evaluation, affective decision-making, and behavioral inhibition, which have been found to be often altered in AN (Rolls, 2004). A previous study has observed increased OFC volume in adolescents with AN (Frank et al., 2013). Furthermore, a multicenter neuroimaging study on AN revealed a positive correlation between gray matter volume in the OFC and the severity of AN symptoms, suggesting that a relatively larger OFC volume in AN is associated with intense food restriction characteristic of AN (Tose et al., 2024). The current GWC finding may offer a microstructural complement to these prior observations, pointing to potential

differences in intracortical myelination or cytoarchitecture that do not necessarily translate into gross morphological indices. The inferior temporal cortex, including the fusiform gyrus, supports high-level visual processing functions such as face and body recognition (Weiner & Zilles, 2016). Aberrant activity in this region has been consistently implicated in altered perceptual and affective responses to body-related stimuli in AN (Suchan et al., 2013). Our finding of increased GWC in this region suggests that such functional alterations may be underpinned by microstructural disruptions at the gray-white boundary, potentially reflecting changes in myelin content, cellular density, or tissue composition. These alterations could contribute in modulating how visual information about the body is encoded and integrated, thereby contributing to persistent body image distortion (Uher et al., 2005).

At a methodological level, the present observations argue for treating GWC as complementary rather than standalone. Pairing it with T1w/T2w myelin mapping, magnetization transfer or myelin-water imaging, and diffusion-based models (e.g., NODDI) could help parse contributions from myelination, neurite architecture, and water content. In this direction, multimodal pipelines are likely required to increase biological specificity and reproducibility. Beyond methods, its clinical relevance remains to be established. Priority questions are best addressed with longitudinal designs—for example, pre/post refeeding and follow-up scans—to test whether baseline GWC predicts weight-restoration trajectories and relapse risk, and whether early GWC change anticipates treatment response. Such designs would also allow mapping individual GWC trajectories and relating them to reward-related and body-processing dimensions, helping to disentangle state- versus trait-like alterations. This study has some limitations that warrant consideration. First, the relatively small sample size may have limited statistical power, particularly in detecting more subtle or spatially diffuse effects, and constrains the generalizability of the findings. Second, the cross-sectional design precludes any causal inference regarding the directionality of observed GWC alterations. Specifically, it remains unclear whether these differences reflect state-related consequences of malnutrition or trait-like neurobiological markers associated with vulnerability to AN. Third, hydration status, a known modulator of T1 signal intensity, was not rigorously standardized across participants. Although all individuals were clinically stable at the time of scanning, subtle differences in hydration or nutritional status may have introduced inter-individual variability in tissue contrast.

Despite these limitations, a strength of this study lies in the use of GWC as a relatively novel morphometric marker in AN. By capturing signal intensity differences at the cortical boundary, GWC integrates microstructural features of both GM and WM, offering a complementary perspective to conventional measures such as CT or volumetry. This approach has the potential to deepen our understanding of the neurobiological underpinnings of AN, particularly in relation to intracortical myelination and tissue integrity.

In conclusion, these findings support the potential utility of GWC as a sensitive and complementary marker of cortical microstructure in AN. Including GWC in future neuroimaging studies may enhance our ability to detect subtle, physiologically meaningful alterations not captured by conventional morphometric indices, ultimately contributing to a more nuanced understanding of cortical alterations in anorexia nervosa.

CRedit authorship contribution statement

Sanberk Ugur: Writing – original draft, Methodology, Formal analysis, Conceptualization. **Christopher R. Madan:** Writing – review & editing, Methodology, Formal analysis. **Valentina Meregalli:** Methodology, Investigation. **Sofia Gentili:** Investigation, Data curation. **Serena Giovannini:** Investigation, Data curation. **Marco Romanelli:** Investigation, Data curation. **Renzo Manara:** Methodology, Data curation. **Angela Favaro:** Writing – review & editing, Supervision, Investigation. **Enrico Collantoni:** Writing – review & editing, Supervision, Methodology, Formal analysis, Data curation, Conceptualization.

Funding

This work was supported by the STARS@UNIPD funding program of the University of Padova, Italy, through the project: EXPLAIN_AN.

References

- American Psychiatric Association. (2013). Diagnostic and Statistical Manual of Mental Disorders. American Psychiatric Association. <https://doi.org/10.1176/appi.books.9780890425596>.
- Chwa, W.J., Tishler, T.A., Raymond, C., Tran, C., Anwar, F., Villablanca, J.P., Ventura, J., Subotnik, K.L., Nuechterlein, K.H., Ellingson, B.M., 2020. Association between cortical volume and gray-white matter contrast with second generation antipsychotic medication exposure in first episode male schizophrenia patients. *Schizophr. Res.* 222, 397–410. <https://doi.org/10.1016/J.SCHRES.2020.03.073>.
- Collantoni, E., Madan, C.R., Meneguzzo, P., Chiappini, I., Tenconi, E., Manara, R., Favaro, A., 2020. Cortical complexity in anorexia nervosa: a fractal dimension analysis. *J. Clin. Med.* 9 (3). <https://doi.org/10.3390/JCM9030833>.
- Collantoni, E., Madan, C.R., Meregalli, V., Meneguzzo, P., Marzola, E., Panero, M., D'Agata, F., Abbate-Daga, G., Tenconi, E., Manara, R., Favaro, A., 2021. Sulcal characteristics patterns and gyrification gradient at different stages of anorexia nervosa: a structural MRI evaluation. *Psychiatry Res. Neuroimaging* 316. <https://doi.org/10.1016/J.PSCYCHRESNS.2021.111350>.
- Collantoni, E., Meneguzzo, P., Tenconi, E., Manara, R., Favaro, A., 2019. Small-world properties of brain morphological characteristics in Anorexia Nervosa. *PLoS One* 14 (5). <https://doi.org/10.1371/JOURNAL.PONE.0216154>.
- Collantoni, E., Pessotto, G., Meregalli, V., Madan, C.R., Miola, A., Cascino, G., Monteleone, A.M., Favaro, A., 2025. Cortical complexity in eating disorders: a systematic review and qualitative synthesis. *Eur. Arch. Psychiatry Clin. Neurosci.* 1–17. <https://doi.org/10.1007/S00406-025-02001-3/FIGURES/2>.
- Drakulich, S., Thiffault, A.C., Olafson, E., Parent, O., Labbe, A., Albaugh, M.D., Khundrakpam, B., Ducharme, S., Evans, A., Chakravarty, M.M., Karama, S., 2021. Maturational trajectories of pericortical contrast in typical brain development. *Neuroimage* 235. <https://doi.org/10.1016/J.NEUROIMAGE.2021.117974>.
- Facca, M., Meregalli, V., Gentili, S., Bertoldo, A., Manara, R., Favaro, A., Collantoni, E., & Affiliations, #. (2025). Local-Global breakdown of Cortical Similarity Networks in Anorexia Nervosa. *MedRxiv*, 2025.10.29.25339093. <https://doi.org/10.1101/2025.10.29.25339093>.
- Fischl, B., 2012. FreeSurfer. *Neuroimage* 62 (2), 774–781. <https://doi.org/10.1016/J.NEUROIMAGE.2012.01.021>.
- Fischl, B., Dale, A.M., 2000. Measuring the thickness of the human cerebral cortex from magnetic resonance images. *PNAS* 97 (20), 11050–11055. <https://doi.org/10.1073/PNAS.200033797>.
- Frank, G.K.W., Shott, M.E., Hagman, J.O., Yang, T.T., 2013. Localized brain volume and white matter integrity alterations in adolescent anorexia nervosa. *J. Am. Acad. Child Adolesc. Psychiatry* 52 (10), 1066–1075.e5. <https://doi.org/10.1016/J.JAAC.2013.07.007/ASSET/010760C9-B6E5-4143-B936-62762CCA58C4/MAIN.ASSETS/GR2.SML>.
- Jørgensen, K.N., Nerland, S., Norbom, L.B., Doan, N.T., Nesvåg, R., Mørch-Johnsen, L., Haukvik, U.K., Melle, I., Andreassen, O.A., Westlye, L.T., Agartz, I., 2016. Increased MRI-based cortical grey/white-matter contrast in sensory and motor regions in schizophrenia and bipolar disorder. *Psychol. Med.* 46 (9), 1971–1985. <https://doi.org/10.1017/S0033291716000593>.
- King, J.A., Frank, G.K.W., Thompson, P.M., Ehrlich, S., 2018. Structural neuroimaging of anorexia nervosa: future directions in the quest for mechanisms underlying dynamic alterations. *Biol. Psychiatry* 83 (3), 224–234. <https://doi.org/10.1016/J.BIOPSYCH.2017.08.011>.
- Lewis, J.D., Evans, A.C., Tohka, J., 2018. T1 white/gray contrast as a predictor of chronological age, and an index of cognitive performance. *Neuroimage* 173, 341–350. <https://doi.org/10.1016/J.NEUROIMAGE.2018.02.050>.
- Madan, C.R., 2018. Age differences in head motion and estimates of cortical morphology. *PeerJ* 2018 (7), e5176.
- Mann, C., Bletsch, A., Andrews, D., Daly, E., Murphy, C., Murphy, D., Ecker, C., 2018. The effect of age on vertex-based measures of the grey-white matter tissue contrast in autism spectrum disorder. *Mol. Autism* 9 (1). <https://doi.org/10.1186/S13229-018-0232-6>.
- Meneguzzo, P., Collantoni, E., Solmi, M., Tenconi, E., Favaro, A., 2019. Anorexia nervosa and diffusion weighted imaging: an open methodological question raised by a systematic review and a fractional anisotropy anatomical likelihood estimation meta-analysis. *Int. J. Eat. Disord.* 52 (11), 1237–1250. <https://doi.org/10.1002/EAT.23160>.
- Rolls, E.T., 2004. The functions of the orbitofrontal cortex. *Brain Cogn.* 55 (1), 11–29. [https://doi.org/10.1016/S0278-2626\(03\)00277-X](https://doi.org/10.1016/S0278-2626(03)00277-X).
- Salat, D.H., Lee, S.Y., van der Kouwe, A.J., Greve, D.N., Fischl, B., Rosas, H.D., 2009. Age-associated alterations in cortical gray and white matter signal intensity and gray to white matter contrast. *Neuroimage* 48 (1), 21–28. <https://doi.org/10.1016/J.NEUROIMAGE.2009.06.074>.
- Seitz, J., Bühren, K., Von Polier, G. G., Heussen, N., Herpertz-Dahlmann, B., & Konrad, K. (2013). Morphological Changes in the Brain of Acutely Ill and Weight-Recovered Patients with Anorexia Nervosa. 42(1), 7–18. <https://doi.org/10.1024/1422-4917/A000265>.
- Suchan, B., Bausser, D.S., Busch, M., Schulte, D., Grönemeyer, D., Herpertz, S., Vocks, S., 2013. Reduced connectivity between the left fusiform body area and the extrastriate

- body area in anorexia nervosa is associated with body image distortion. *Behav. Brain Res.* 241 (1), 80–85. <https://doi.org/10.1016/J.BBR.2012.12.002>.
- Tose, K., Takamura, T., Isobe, M., Hirano, Y., Sato, Y., Kodama, N., Yoshihara, K., Maikusa, N., Moriguchi, Y., Noda, T., Mishima, R., Kawabata, M., Noma, S., Takakura, S., Gondo, M., Kakeda, S., Takahashi, M., Ide, S., Adachi, H., ... Sekiguchi, A. (2024). Systematic reduction of gray matter volume in anorexia nervosa, but relative enlargement with clinical symptoms in the prefrontal and posterior insular cortices: a multicenter neuroimaging study. *Molecular Psychiatry* 29:4, 29(4), 891–901. <https://doi.org/10.1038/s41380-023-02378-4>.
- Treasure, J., Duarte, T.A., Schmidt, U., 2020. Eating disorders. *Lancet (London, England)* 395 (10227), 899–911. [https://doi.org/10.1016/S0140-6736\(20\)30059-3](https://doi.org/10.1016/S0140-6736(20)30059-3).
- Uher, R., Murphy, T., Friederich, H.C., Dalgleish, T., Brammer, M.J., Giampietro, V., Phillips, M.L., Andrew, C.M., Ng, V.W., Williams, S.C.R., Campbell, I.C., Treasure, J., 2005. Functional neuroanatomy of body shape perception in healthy and eating-disordered women. *Biol. Psychiatry* 58 (12), 990–997. <https://doi.org/10.1016/j.biopsych.2005.06.001>.
- Walton, E., Bernardoni, F., Batury, V.L., Bahnsen, K., Larivière, S., Abbate-Daga, G., Andres-Perpiña, S., Bang, L., Bischoff-Grethe, A., Brooks, S.J., Campbell, I.C., Cascino, G., Castro-Fornieles, J., Collantoni, E., D'Agata, F., Dahmen, B., Danner, U. N., Favaro, A., Feusner, J.D., Ehrlich, S., 2022. Brain structure in acutely underweight and partially weight-restored individuals with anorexia nervosa - a coordinated analysis by the ENIGMA eating disorders working group. *Biol. Psychiatry* 92 (9), 730. <https://doi.org/10.1016/J.BIOPSYCH.2022.04.022>.
- Weiner, K.S., Zilles, K., 2016. The anatomical and functional specialization of the fusiform gyrus. *Neuropsychologia* 83, 48–62. <https://doi.org/10.1016/J.NEUropsychologia.2015.06.033>.
- White, T., Su, S., Schmidt, M., Kao, C.Y., Sapiro, G., 2010. The development of gyrification in childhood and adolescence. *Brain Cogn.* 72 (1), 36–45. <https://doi.org/10.1016/J.BANDC.2009.10.009>.
- Worsley, K., Taylor, J., Carbonell, F., Chung, M., Duerden, E., Bernhardt, B., Lyttelton, O., Boucher, M., Evans, A., 2009. SurfStat: a Matlab toolbox for the statistical analysis of univariate and multivariate surface and volumetric data using linear mixed effects models and random field theory. *Neuroimage* 47, S102. [https://doi.org/10.1016/S1053-8119\(09\)70882-1](https://doi.org/10.1016/S1053-8119(09)70882-1).